Experimental Gerontology 179 (2023) 112233

Contents lists available at ScienceDirect

Experimental Gerontology

journal homepage: www.elsevier.com/locate/expgero

Senescent adipocytes as potential effectors of muscle cells dysfunction: An *in vitro* model

Zoico Elena [a], Saatchi Tanaz [a,*], Nori Nicole [a], Mazzali Gloria [a], Rizzatti Vanni [b], Pizzi Eleonora [b], Fantin Francesco [a], Giani Anna [a], Urbani Silvia [a], Zamboni Mauro [b]

[a] Department of Medicine, Geriatric Section, University of Verona, Verona, Italy
[b] Department of Surgery, Dentistry, Pediatrics and Gynecology, University of Verona, Verona, Italy

ARTICLE INFO

Section Editor: Christiaan Leeuwenburgh

Keywords:
Aging
Adipose tissue
Skeletal muscle
Senescence
Myostatin

ABSTRACT

Recently, there has been a growing body of evidence showing a negative effect of the white adipose tissue (WAT) dysfunction on the skeletal muscle function and quality. However, little is known about the effects of senescent adipocytes on muscle cells.

Therefore, to explore potential mechanisms involved in age-related loss of muscle mass and function, we performed an *in vitro* experiment using conditioned medium obtained from cultures of mature and aged 3 T3-L1 adipocytes, as well as from cultures of dysfunctional adipocytes exposed to oxidative stress or high insulin doses, to treat C2C12 myocytes.

The results from morphological measures indicated a significant decrease in diameter and fusion index of myotubes after treatment with medium of aged or stressed adipocytes. Aged and stressed adipocytes presented different morphological characteristics as well as a different gene expression profile of proinflammatory cytokines and ROS production. In myocytes treated with different adipocytes' conditioned media, we demonstrated a significant reduction of gene expression of myogenic differentiation markers as well as a significant increase of genes involved in atrophy. Finally, a significant reduction in protein synthesis as well as a significant increase of myostatin was found in muscle cells treated with medium of aged or stressed adipocytes compared to controls.

In conclusion, these preliminary results suggest that aged adipocytes could influence negatively trophism, function and regenerative capacity of myocytes by a paracrine network of signaling.

1. Introduction

White Adipose tissue (WAT), as the largest energy depot and endocrine organ in humans, is essential for maintenance of systemic glucose, lipids, and energy homeostasis but its functions decline with aging (Palmer and Kirkland, 2016; Zamboni et al., 2021). WAT undergoes to several changes with aging, with a decrease in preadipocytes' differentiation capacity, increase of senescent cells with a senescence-associated secretory phenotype (SASP), increase in pro-inflammatory cytokines and immune cells infiltration, reduction in vascularization and increase in fibrosis (Tchkonia et al., 2010). The age-related changes in WAT are responsible for a systemic low state of inflammation, that is called "inflammageing" (Franceschi and Campisi, 2014), which may affect the function of other organs including muscle tissue (Pedersen, 2011).

Muscle changes in mass and quality that occur with aging, and that are at the base of the definition of Sarcopenia (Morley et al., 2001), are responsible for an increased risk of frailty, functional impairment and disability in the elderly. Aging of skeletal muscle is characterized by an impaired muscle quality with an increase in muscle fat infiltration, also called myosteatosis, and by an increase in fibrous connective tissue and an impairment in muscle regenerative potential, leading to myofibrosis (Zoico et al., 2013). In particular, fat infiltration in the muscle, within muscle cells and/between muscle fibers, increases with age and adiposity (Gallagher et al., 2005; Goodpaster et al., 2001) and is strongly related to metabolic abnormalities (Petersen et al., 2003), and reduced muscle strength and performance (Visser et al., 2005).

In obesity, muscle fat infiltration is linked to mitochondrial dysfunction, increased oxidative stress, impaired insulin sensitivity and enhanced secretion of pro-inflammatory myokines capable of inducing muscle dysfunction in a paracrine or autocrine manner (Kalinkovich and Livshits, 2017). To our knowledge, this interplay between adipocytes and myocytes has been directly investigated in obese patients or in

* Corresponding author.
E-mail address: tanaz.saatchi@univr.it (S. Tanaz).

https://doi.org/10.1016/j.exger.2023.112233
Received 3 November 2022; Received in revised form 31 May 2023; Accepted 11 June 2023
Available online 19 June 2023

obesity animal models through a few *in vivo* and *in vitro* studies, supporting a role for dysfunctional adipocytes as potential effectors of muscle cell dysfunction (Wilhelmsen et al., 2021). Pellegrinelli et al. (2015), provided evidence for a cross-talk between human obese adipocytes and muscle cells, showing that the secretome of visceral adipocytes from obese patients decreased the expression of contractile proteins and induced muscle atrophy, decreasing gene expression of factors involved in myogenesis and muscle contractility. *In vitro*, conditioned medium from differentiated human adipocytes has been shown to impair the insulin pathway in myocytes (Sell et al., 2008) as well as changes in proteins expression (Sell et al., 2008).

During aging, muscle fat accumulation, and in particular the accumulation of senescent cells, has been proposed to drive, through SASP and thus through local inflammation, muscle dysfunction (Wilhelmsen et al., 2021). However, to our knowledge, no study has directly investigated if WAT senescence may be implicated in the pathogenesis of muscle dysfunction and Sarcopenia in the elderly.

Several cytokines and molecules, of both adipose and muscular origin, have been hypothesized to be the mediators of the cross-talk between adipose and muscle, as the more investigated leptin, adiponectin, resistin, IL-15 and myostatin as well as some emerging and less known microRNAs (Wilhelmsen et al., 2021). However, the specific factors involved in the cross-talk between senescent adipocytes and muscle cells and the pathways regulated are still not completely known. In a previous *in vitro* study, we observed a decrease in proadipogenic signals, genes related to glucose metabolism and cytoskeleton maintenance, and adiponectin levels, accompanied by an increase in inflammatory cytokines in aging adipocytes (Zoico et al., 2010).

As the role of senescent and dysfunctional adipocytes on muscle is still not completely explored, the aim of this preliminary study was to test *in vitro* the effects of different model of aged and stressed adipocytes on trophysm, function and regenerative capacity of myocytes. In particular, in an indirect co-culture system, we exposed muscle cells to conditioned medium obtained from cultures of mature adipocytes or aged and dysfunctional adipocytes. Prolonged cultures exposition to oxidative stress as well as to high insulin doses were used as models of dysfunctional adipocytes.

2. Materials and methods

2.1. Adipocyte cell culture: 3 T3-L1 cell line

Murine 3 T3-L1 pre-adipocytes (ECACC-Sigma-Aldrich) were cultured at 37 °C in a 5 % CO2 atmosphere using D-MEM/GlutaMAX (Gibco) culture medium. The culture medium consisted of Dulbecco's modified Eagle medium (D-MEM) with 2 mM L-glutamine, supplemented with 10 % fetal bovine serum (FBS) and 1 % antibiotic-antimycotic solution (Sigma). Once the cells reached 85 %–90 % confluence after three days, they were detached using a 0.5 mg/ml trypsin/EDTA (Gibco) solution and washed with PBS. To determine the number of viable cells, 50 μl of resuspended cells were stained with 0.04 % Trypan Blue for 2 min and examined under a microscope. The Countess Automated Cell Counter (Invitrogen) was used for cell counting. Subsequently, 3000 cells per well were seeded in 6-well plates (Becton Dickinson) containing pre-sterilized slides (Menzel-Glaser Thermo Scientific). Two days after reaching confluence, which corresponded to Post Induction Day (PID) 0, cell differentiation was induced using D-MEM/F12 medium supplemented with 10 % FBS, 1 % antibiotic-antimycotic solution, 0.2 mM 3-isobutyl-1-methylxanthine (IBMX), 10 nM rosiglitazone, 1 μM dexamethasone, and 1.72 μM insulin (Sigma). On PID3, the differentiation medium was replaced with adipocyte maintenance medium (AMM) consisting of D-MEM/F12 supplemented with 10 % FBS, 1 % antibiotic-antimycotic solution, and 1.72 μM insulin. The cells were cultured in this medium until PID 5 when it was switched to a maintenance medium containing insulin at a physiological concentration (10 nM) for an additional 2 days. On PID 7, the medium was changed again by removing insulin, and the cells were cultured in a medium consisting solely of D-MEM/F12, 1 % antibiotic-antimycotic solution, and 10 % FBS.

Conditioned medium (CM) was obtained from 3 T3-L1 cells under various experimental conditions and utilized for culturing C2C12 cells in an indirect co-culture system. Specifically, CM was derived from adipocytes at PID10, which were considered mature adipocytes based on previous studies (Yu and Zhu, 2004; Zoico et al., 2010) (Fig. 1).

Additionally, CM was obtained from adipocyte cultures extended until PID18, displaying morphological and functional features characteristic of senescent adipocytes as previously described (Zoico et al., 2019) (Fig. 1). Regarding the conditioned media of these cells, from PID10 to PID15, the medium was changed every two days with D-MEM/F12 supplemented with 1 % antibiotic-antimycotic, 10 % FBS, and 10 nM insulin. On PID15, the medium was further modified by removing insulin, and the cells were cultured in a medium composed solely of D-MEM/F12, 1 % antibiotic-antimycotic solution, and 10 % FBS until PID18 for subsequent medium collection.

Moreover, conditioned medium (CM) was obtained from two additional models of stressed adipocytes, which were generated by exposing the cells to oxidative stress using hydrogen peroxide (PID10 H2O2) and by treating them with high doses of insulin to induce insulin resistance (PID10 IR) (Fig. 1). In more detail, from PID 5 to PID 7, adipocytes were treated with 150 μM H2O2 (30 % w/w in H2O) (Sigma) in D-MEM/F12 supplemented with 1 % antibiotic-antimycotic solution and 10 nM insulin for 3 h each day. Subsequently, the cells were washed with PBS and incubated in D-MEM/F12 containing 1 % antibiotic-antimycotic, 10 % FBS, and 10 nM insulin. After the final treatment on PID7, the cells were washed with PBS and incubated with an insulin-free 10 % FBS medium until PID10 for subsequent collection (Zoico et al., 2019) (Fig. 1).

In relation to the conditioned medium (CM) obtained from insulin-resistant adipocytes, differentiated adipocytes were exposed to a 10 uM insulin treatment in a maintenance medium without fetal bovine serum (FBS) during the final 16 h of PID9. On PID10, the cells were rinsed with PBS and incubated in a medium devoid of both FBS and insulin for 6 h prior to collecting the conditioned medium (Pinel et al., 2018) (Fig. 1).

2.2. Myoblast cell culture: C2C12 cell line

Murine C2C12 myoblasts (ATCC) were cultured in complete D-MEM/GlutaMAX medium, which consisted of Dulbecco's Modified Eagle Medium (high glucose) supplemented with 10 % FBS and 1 % antibiotic antimycotic solution. The cells were maintained at 37 °C in a 5 % CO2 atmosphere.

Upon reaching 80 % confluence, the cells were detached using trypsin/EDTA and subsequently stained with 0.5 % Trypan Blue for cell counting. A total of 4800 cells were seeded per well in 6-well plates (Falcon, BD Bioscience), each containing a pre-sterilized slide. The cells were incubated with D-MEM/GlutaMAX medium supplemented with 10 % FBS and 1 % antibiotic antimycotic solution.

Two days after seeding, which corresponds to Post Induction Day (PID) 0, when the cells reached 80 % confluence, differentiation of the myoblasts was induced by using a D-MEM medium supplemented with 2 % FBS and 1 % antibiotic antimycotic solution. The progression of differentiation was assessed through optical microscopy on PID 0, 3, 5, and 7, with the formation of syncytial myotubes observed on PID 3.

To evaluate the impact of senescent or dysfunctional adipocytes, murine C2C12 cells were treated with conditioned medium (CM) collected from 3 T3-L1 adipocyte cultures under different experimental conditions. This involved replacing 50 % of the myocyte culture medium with the CM obtained from adipocytes at various stages (mature at PID 10, aged until PID 18, stressed with H2O2, and insulin resistant). The treatments were performed at PID 5 and PID 7, each lasting for 48 h. On PID 9, the cells were collected for further analysis.

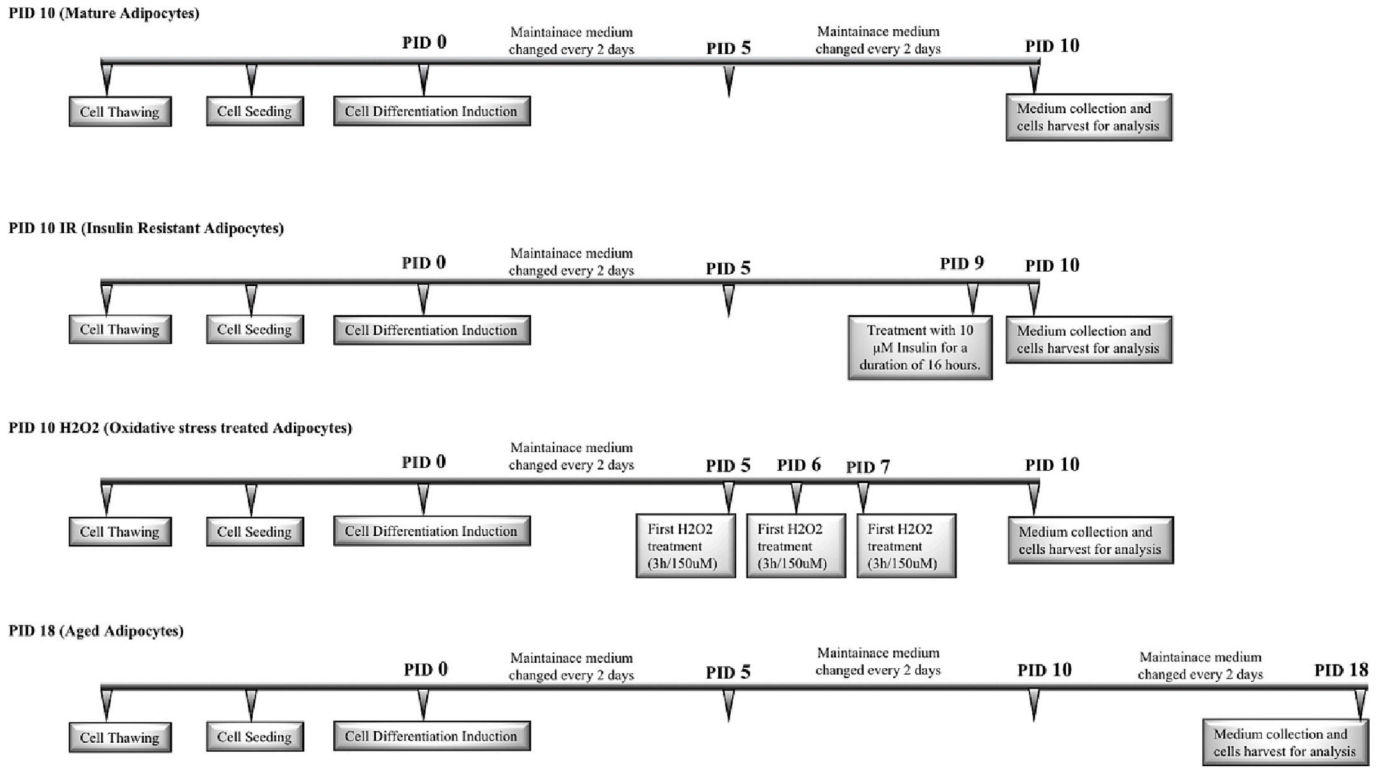

Fig. 1. A diagram illustrating the various experimental conditions for generating different models of stressed adipocytes. PID: post induction day.

2.3. Adipocyte morphology evaluation

Following a rinse with 0.1 M pH 7.4 phosphate-buffered saline (PBS), the cell cultures were fixed using 10 % neutral buffered formalin for 10 min. Subsequently, the cells were washed with sterile double-distilled water and stained with a filtered, ready-to-use Oil Red O solution (Bio-Optica, Milano, Italy) for 20 min at room temperature. After another round of washing with sterile double-distilled water, the cells were stained with Mayer's Hematoxylin (Bio-Optica, Milano, Italy) ready-to-use solution for 1 min at room temperature, followed by a final wash with sterile double-distilled water. Slides were then treated with Aqueous Mount Quick Medium (Bio-Optica, Milano, Italy).

The cellular observations were conducted using an EVOS FL Auto Cell Imaging System with EVOS Onstage Incubator (Thermo Fisher Scientific, USA) photomicroscope at 20× and 40× magnification. Image analysis was performed using ImageJ software version 1.51n (NIH, Bethesda, MD, USA). The analysis included cell counting within 10 representative fields (20× magnification, number of cells expressed per mm^2) and the measurement of the area of 50 randomly selected cells (20× magnification; area expressed in μm^2).

2.4. ROS analysis

Intracellular ROS generation was assessed using the Image-iT™ LIVE Green Reactive Oxygen Species (ROS) Detection Kit (Thermo Fisher Scientific, USA). Following treatment according to the experimental conditions, cells were washed once with 1 ml of warm HBSS/Ca/Mg and incubated with a 25 µM carboxy-H2DCFDA working solution for 30 min at 37 °C, protected from light. During the last 5 min of incubation, Hoechst 33342 was added at a final concentration of 1.0 µM to the carboxy-H2DCFDA staining solution. Subsequently, the cells were gently washed three times with warm HBSS/Ca/Mg, and the coverslip was mounted using Antifade Mounting Medium - Prolong Fluorescence (Boster Biological Technology, USA).

Cellular observations were performed using an EVOS FL Auto Cell Imaging System with EVOS Onstage Incubator (Thermo Fisher Scientific, USA) photomicroscope at 20× and 40× magnification. Image analysis was conducted using ImageJ software version 1.51n (NIH, Bethesda, MD, USA). The mean fluorescence intensity for each treatment was calculated based on 50 ROS-positive cells observed at 20× magnification, by computing the integrated density (ID). The background signal was obtained by measuring the fluorescence intensity of regions outside the cells. The corrected total cell fluorescence (CTCF) was then determined by subtracting the background signal from the ID (CTCF = ID - background).

2.5. Myocyte morphological evaluation and assessment of diameters and fusion index

After being washed with PBS, myocytes were fixed in 10 % neutral buffered formalin for 1 min. They were then washed twice with sterile double-distilled water and stained with Oil Red O filtered solution (Bio-Optica) for 20 min at room temperature (RT). Subsequently, the cells were washed and stained with Meyer's hematoxylin solution (Bio-Optica) for 1 min at RT, followed by another wash. The slides were then treated with Aqueous Mount Quick Medium (Bio-Optica). Myocyte observation and image acquisition were performed using an EVOS FL Auto Cell Imaging System with EVOS Onstage Incubator microscope (Thermo Fisher Scientific), both at 20× and 40× magnification. The diameter of myotubes was calculated from 10 randomly selected images at 40× magnification for each experimental condition, evaluating > 50 myotubes for each condition. The fusion index or myotube formation index was expressed as the ratio of nuclei in myosin heavy chain IIb (MyHC-IIb) positive multinucleated cells with ≥ 3 nuclei to the total number of stained nuclei present in the analyzed area. The fusion index was calculated from 5 images at 40× magnification, analyzing at least 1000 nuclei. The analysis was performed using ImageJ program (version 1.52o).

2.6. Viability of C2C12 cells

The viability of myocytes in response to stressed adipocytes was evaluated using the 3-(4,5-dimethylthiazol-2-yl)-2,5-diphenyltetrazolium bromide (MTT) assay kit from Sigma-Aldrich. This assay kit was employed to specifically investigate the effect of different conditioned media (CMs) on muscle cell viability, providing insights into their potential impact on muscle cell number.

Cells were seeded at a concentration of 1500 cells/well in a 96-well microplate and treated as described in Section 2.2. On PID 8, the MTT labeling reagent was added to each well at a final concentration of 0.5 mg/ml. The microplate was then incubated at 37 °C in a 5 % CO2 atmosphere for 4 h. After incubation, a solubilization solution was added to dissolve the MTT formazan crystals, and the microplate was left overnight in the incubator at 37 °C in a 5 % CO2 atmosphere. Finally, the absorbance of each well was measured at 550 nm using a PerkinElmer's Victor X4 microplate reader. Wells without cells (medium only) containing the MTT solution were used as blanks for appropriate background subtraction. The data are expressed as a percentage of cell viability compared to the control, calculated as 100 × (absorbance of sample treated cells - absorbance of blank samples) / (absorbance of control cells) (Supplementary Fig. S1).

2.7. RNA extraction, retro-transcription (RT-PCR) and evaluation of gene expression (real-time PCR)

Total RNA was extracted using miRNeasy Mini Kit (Qiagen) as previously described (Zoico et al., 2010). RT-PCR reaction was performed using First Strand cDNA Synthesis Kit (Origen). The adopted protocol consisted of 5 min at 25 °C, 20 min at 46 °C and 1 min at 95 °C. mRNA amplification was carried out employing a CFX96 Real-Time machine (Bio-Rad) using SsoAdvanced Universal SYBR Green Supermix following the producer protocol (Bio-Rad). A Real-time PCR reaction has been performed, amplifying 50 ng of cDNA in a 20 ul volume for 40 cycles at the following conditions: 95 °C for 5 s and 60 °C for 30 s.

The primer pairs have been designed to amplify 150 bp DNA fragments: Resistin (FW, 5′ - TCA CTTTTCACCTCTGTGGATATGAT- 3′; RV, 5′-TGCCCCAGGTGGTGTAAA -3′), IL-6 (FW, 5′-CCTCTGGTCTTCTGGAGTACC -3′; RV, 5′- ACTCCTTCTGTGACTCCAGC-3′), TNF-alpha (FW, 5′- ATGAGCACAGAAAGCATGA -3′; RV, 5′- AGTAGACAGAAGAGCGTGGT -3′), GLUT4 (FW, 5′- CAGCTCTCAGGCATCAAT-3′; RV, 5′- TCTACTAAGAGCACCGAG -3′), MCP1 (FW, 5′-CTTCCTCCACCACCATGCA -3′; RV, 5′- CCAGCCGGCAACTGTGA-3′), MHC-IIb (FW,5′-CTTTGCTTACGTCAGTCAAGGT-3′; RV,5′-AGCGCCTGTGAGCTTGTAAA-3′), MYOSTATIN (FW,5′ CCAGGACCAGGAGAAGATGG-3′; RV,5′-GGATTCCGTGGAGTGCTCAT-3′), MuRF1 (FW, 5′-TGCCTACTTGCTCCTTGTGC-3′;RV,5′-CACCAGCATGGAGATGCAGT-3′), CCN-2 (FW, 5′- CCACCCGAGTTACCAATGAC-3′; RV, 5′-GTGCAGCCAGAAAGCTCA-3′), COL1A1 (FW, 5′-ATGTTCAGCTTTGTGGACCT-3′; RV, 5′-CAGCTGACTTCAGGGATGT-3′), GADPH (FW, 5′- ACA GTC CAT GCC ATC ACT GCC -3′; RV, 5′- GCC TGC TTC ACC ACC TTC TTG -3′). GAPDH has been used as an internal control to normalize data. The variation of GAPDH expression is illustrated in (Supplementary Fig. 2). PCR results were analyzed through Bio-Rad iQ™ optical system software. Each analysis has been performed at least in duplicate, and gene expression levels were calculated using the following formula: $2^{-\Delta\Delta Ct}$.

2.8. Western blot (WB) protein analysis

Myocytes were suspended in RIPA lysis buffer (Thermo Fisher Scientific) supplemented with a complete protease inhibitor cocktail (Roche). The samples were centrifuged at 20,000*g* for 10 min at 4 °C, and the supernatant was collected. The protein concentration of each sample was determined using the Bradford protein assay (Bio-Rad) by measuring the absorbance at 595 nm. Protein quantification was performed by interpolating the obtained absorbance values onto a standard calibration curve generated with BSA. For each sample, a total protein amount of 25 μg was loaded onto a 7.5 % SDS polyacrylamide gel. Electrophoresis was conducted at 100 V for 90 min in a 0.1 % SDS running buffer. Subsequently, the proteins were transferred from the gel onto a PVDF membrane (Immobilon P, Millipore, Bedford MA) using a Mini Protean II TM System (Bio-Rad) with a constant potential of 100 V. The membrane was blotted for 1 h on ice using a buffer containing 10 mM Tris-HCl (pH 8.3), 192 mM glycine, and 10 % methanol. Afterward, the membrane was incubated at room temperature for 1 h in a blocking solution composed of 5 % BSA in TBST solution (10 mM Tris-HCl, pH 7.5, 100 mM NaCl, and 0.1 % Tween20). Overnight incubation at 4 °C with agitation was performed using the primary antibodies diluted 1:1000 in the blocking solution. The primary antibodies used were Anti-GDF8/myostatin Antibody (rabbit anti-mouse; Abcam) and Anti-α-tubulin Antibody as the internal control (rabbit anti-mouse; Cell Signaling). The membrane was then incubated with a secondary anti-rabbit HRP-linked antibody (Cell Signaling) diluted 1:4000 in the blocking solution for 1 h with agitation at room temperature. Before and after this step, the membrane was washed three times for 10 min with TBST. Chemiluminescence detection was performed using the ECL Select Western Blotting Detection Reagent Kit (GE Healthcare) following the supplier's recommendations. The antigen-antibody complexes were visualized using the Alliance Q9 Advanced chemidoc imaging platform (Uvitec).

2.9. Analysis of protein synthesis via Puromycin assay: SUnSET method

A 1 mM solution of puromycin (Puromycin Dihydrochloride, Sigma Aldrich) in PBS was prepared and added directly to each well containing cells in the different experimental conditions, achieving a final concentration of 1 μM. The plates were then incubated at 37 °C for 30 min. Subsequently, cells were washed twice with PBS and lysed to collect proteins as described previously. For each sample, a total of 25 μg of proteins was loaded onto a 10 % SDS polyacrylamide gel, and Western blotting (WB) was performed as described earlier.

The membrane was incubated overnight at 4 °C with gentle agitation in a blocking solution of 1 % BSA in TBST, containing the primary Anti-Puromycin antibody (Sigma Aldrich) diluted 1:5000. After 30 min of washing with TBST, the membrane was incubated for 1 h at room temperature with the secondary Peroxidase AffiniPure Goat Anti-Mouse IgG antibody (Jackson ImmunoResearch) diluted 1:50,000 in blocking solution containing 5 % BSA. Following another 30-minute wash with TBST, the bands on the membrane were visualized using enhanced chemiluminescence (ECL) reagent (Cytiva Amersham™ ECL Select™ Western Blotting Detection Reagent).

After capturing the appropriate images, the membranes were stained with Coomassie Brilliant Blue R-250 (CBB) (Bio-Rad) to ensure uniform loading in all lanes. Densitometric measurements were performed by calculating the density of each entire lane, covering the entire molecular weight range of puromycin-labeled peptides, using ImageJ software for both puromycin and CBB staining.

2.10. Statistical analysis

Data are presented as mean ± SD from three to five independent experiments as specified in all figure legends. The data distribution was checked in the term of normality by Shapiro-Wilk test. Differences between treatment groups and controls were evaluated by One-way ANOVA test for independent samples. A p-value < 0.05 was used to determine statistical significance. All statistical analyses were performed with GraphPad Prism 9.0.0.

3. Results

3.1. Morphological and functional characterization of the different models of stressed and aged adipocytes

In this *in vitro* study, we characterized mature and aged 3 T3-L1 adipocytes, as well as adipocytes exposed to oxidative stress or high insulin doses, from a morphological perspective using hematoxylin and eosin staining and Oil Red O staining (Fig. 2). The morphological changes of adipocytes in culture were observed with progressive alterations in diameter and area from PID 10 to PID 18 adipocytes, consistent with previous findings (Zoico et al., 2019). Adipocytes exposed to high insulin doses (PID 10 IR) exhibited an intermediate phenotype (Fig. 2). Adipocytes treated with H2O2 (PID 10 H2O2) did not show significantly different morphological characteristics compared to mature adipocytes (PID 10), although they exhibited higher levels of ROS production, as detected by immunohistochemistry (Fig. 2).

Fig. 3 presents the gene expression profile of aged and stressed adipocytes. The expression of key pro-inflammatory cytokines such as IL-6, TNF-alpha, and MCP-1 was significantly higher in adipocytes exposed to oxidative stress (PID 10 H2O2) compared to mature adipocytes (PID 10). There was also a non-significant increase in expression observed in aged adipocytes (PID 18), consistent with previous findings (Zoico et al., 2019). Insulin-resistant adipocytes (PID 10 IR) exhibited significantly lower expression of GLUT4, more pronounced than in aged adipocytes or adipocytes exposed to oxidative stress (Fig. 3).

3.2. Morphological changes of C2C12 myocytes treated with conditioned medium of 3T3L1 adipocytes

In this *in vitro* study, C2C12 myocytes were first characterized by a morphological point of view by using hematoxylin and eosin and also Oil Red O staining to evaluate the main differences between myocytes treated with conditioned medium from adipocytes in the different experimental conditions, in particular, from mature adipocytes (PID10), aged adipocytes (PID18), adipocytes exposed to oxidative stress (PID10 H2O2) as well to high insulin doses (PID 10 IR) (Fig. 4, A).

The diameter of the myotubes significantly decreased in cultures treated with the medium of aged adipocytes (PID18; $p < 0,05$), of adipocytes exposed to oxidative stress (PID10 H2O2; $p < 0.05$) and insulin resistant adipocytes (PID10 IR; $p < 0.05$) compared to the control (Fig. 4, B). No significant difference was detected in the diameter of C2C12 cells treated with mature adipocyte medium at PID10 compared to control (Fig. 4, B).

In the different experimental conditions to evaluate the differentiation capacity of myoblasts, the fusion index, or myotube formation index, was then determined (Fig. 5, A). The fusion index was significantly decreased in C2C12 cells after treatment with the conditioned medium of aged adipocytes (PID 18; $p < 0,01$), mature adipocytes subjected to oxidative stress (PID10 H2O2; $p < 0,05$) and insulin-resistant adipocytes (PID10 IR; $p < 0,05$) compared to control (Fig. 5, B). There was no significant difference in the fusion index between the control and the treatment with mature adipocyte medium (PID10) (Fig. 5, B).

3.3. Modulation of genes expression in C2C12 myocytes treated with conditioned medium of 3T3L1 adipocytes

To explore the functional modifications of C2C12 myocytes treated with the conditioned medium of 3 T3-L1 adipocytes in the different experimental conditions, we evaluated mRNA expression of different genes involved in muscle differentiation (MyHC-IIb), in muscle atrophy (MuRF1) and fibrosis (CCN2, COL1A1).

The pathways regulating muscle atrophy were explored by the evaluation of the gene expression of MuRF1, involved in muscle catabolism (Fig. 6). In particular, the expression of MuRF1 was significantly augmented in myocytes treated with medium collected from aged adipocytes (PID 18; $p < 0,05$) as well as from adipocytes in IR condition (PID10 IR; $p < 0,05$) comparing to control condition. Regarding the gene expression of a marker of myogenic differentiation, we observed a significant reduction in myosin heavy chain (MyHC-IIb) gene expression after treatment with all conditioned media from aged or stressed adipocytes compared to control (Fig. 6). Finally, to explore pathways potentially involved in the modulation of muscle fibrosis we evaluated

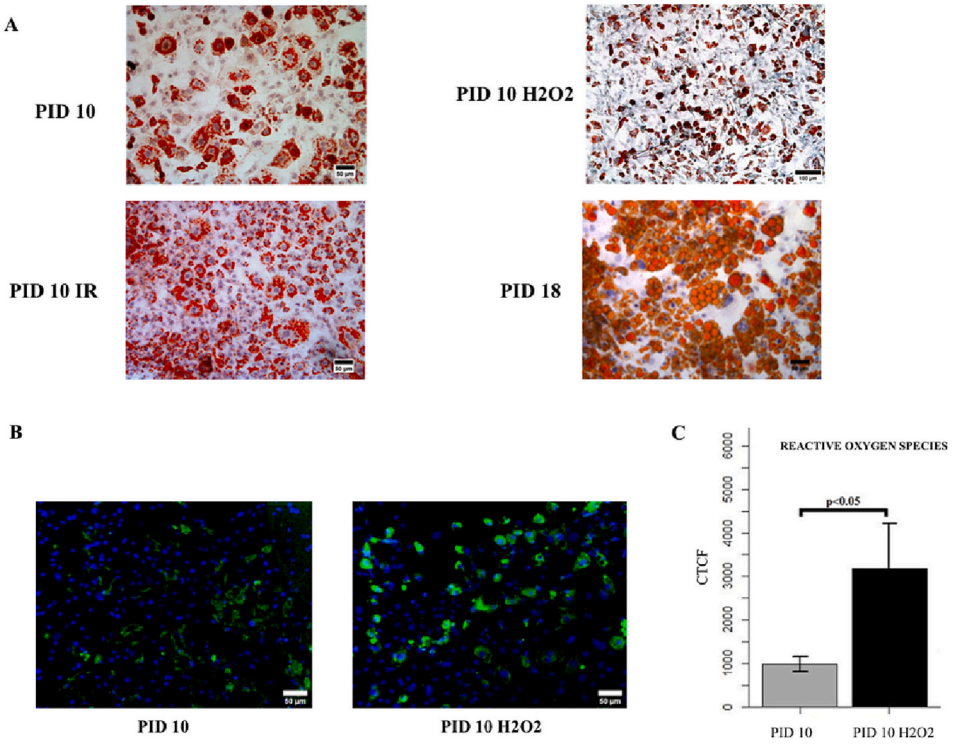

Fig. 2. Morphological characteristics of stressed and aged adipocytes and detection of reactive oxygen species (ROS) through immunofluorescence in adult and treated adipocytes with H2O2 at PID 10. A) Adipocytes treated under different conditions were stained with Oil Red O and Hematoxylin. These conditions included adult adipocytes (PID 10), adipocytes treated with reactive oxygen species (PID 10 H2O2), insulin-resistant adipocytes (PID 10 IR), and aged adipocytes (PID18). B) Significant images of intracellular ROS accumulation (green) in adult adipocytes (PID 10) and adipocytes treated with reactive oxygen species (PID 10 H2O2) are shown. (A, B: scale bar = 50 μm). C) Quantification of intracellular ROS in adult adipocytes (PID 10) and adipocytes treated with reactive oxygen species (PID 10 H2O2). Data are presented as mean ± SD from three independent experiments. *$p < 0.05$ *vs.* the control. PID: post induction day. CTCF: Corrected Total Cell Fluorescence. (For interpretation of the references to colour in this figure legend, the reader is referred to the web version of this article.)

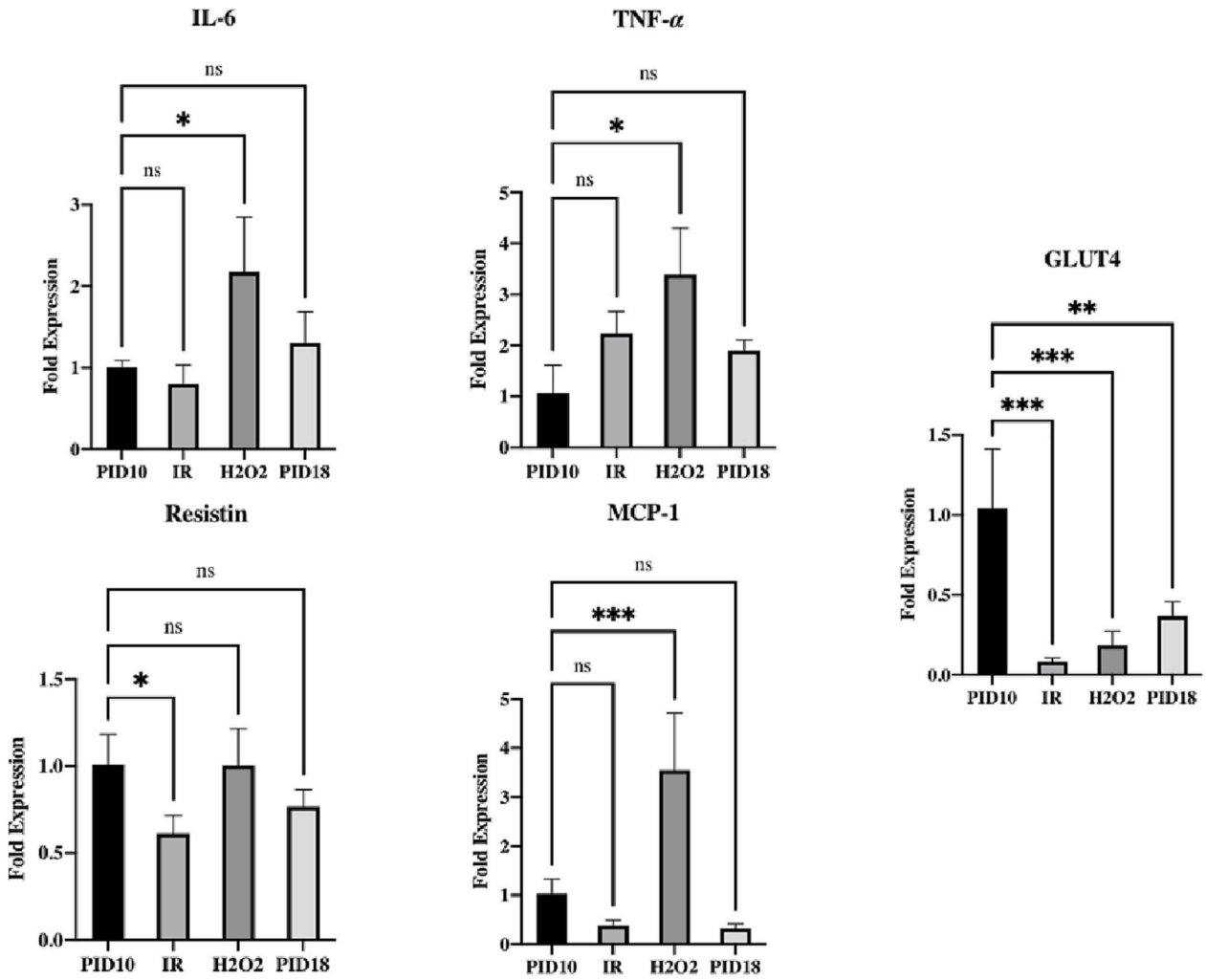

Fig. 3. Gene expression analysis by RT-PCR of key genes involved in pro-inflammatory cytokine production and the gene associated with the insulin signaling pathway in treated adipocytes under different experimental conditions. The expression levels of these genes were measured to characterize the inflammatory and insulin resistance state of stressed and aged adipocytes including: Adult adipocytes (PID10), adipocytes treated with reactive oxygen species (H2O2), insulin resistant adipocytes (IR) and aged adipocytes (PID18). Data are presented as mean ± SD from three to five independent experiments. $^{*}p < 0.05$, $^{**}p < 0.01$, $^{***}p < 0.001$ *vs.* the control, ns: Not Significant. PID: post induction day; IL-6: Interleukin-6; TNF-alpha: Tumor necrosis factor-alpha; MCP-1: Monocyte chemoattractant protein-1; GLUT4: Glucose transporter 4.

the gene expression of CCN-2 and COL1A1 but unfortunately, we did not find any significant modulation of these genes in our experimental model (Supplementary Fig. 3).

3.4. Analysis of the protein synthesis in C2C12 myocytes treated with conditioned medium of 3 T3-L1 adipocytes

To dynamically measure protein synthesis in C2C12 myocytes in the different experimental conditions, we used the assay of the incorporation of puromycin with the SUnSET protocol (Fig. 7). This method revealed a significant reduction in protein synthesis in all the experimental conditions compared to control, when myocytes were exposed to conditioned medium collected from aged or stressed adipocytes (Fig. 7).

3.5. Modulation of myostatin in C2C12 myocytes treated with conditioned medium of 3 T3-L1 adipocytes

Myostatin is a factor implicated in the regulation of muscle mass, determining its atrophy through activation of catabolic pathways, inhibition of protein synthesis and impairment of myoblasts differentiation, as well as in muscle fibrosis. We studied its modulation in myocytes in the different experimental conditions through RT-PCR and WB analyses.

The gene expression of myostatin was significantly increased in myocytes treated with the medium of aged adipocytes (PID18; $p < 0{,}001$) as well as in myocytes treated with conditioned medium from insulin resistant adipocytes (PID 10 IR; $p < 0{,}001$) or from adipocytes exposed to oxidative stress (PID 10 H2O2; $p < 0{,}05$) compared to control (Fig. 8, A).

These data were further reinforced by a WB analysis of myostatin in C2C12 cells treated with medium from adipocytes in the different experimental conditions (Fig. 8, B), observing an increase in myostatin protein in C2C12 cells treated with conditioned medium from aged (PID 18; $p < 0{,}05$), as well as from stressed adipocytes treated with H2O2 (PID 10 H2O2; $p < 0{,}01$) compared to control (Fig. 8, B).

4. Discussion

This preliminary *in vitro* study evaluated, through an indirect co-culture system morphological and functional changes of myocytes after exposure to conditioned medium from adipocytes in different experimental conditions, focusing on the effects caused by aged or dysfunctional adipocytes to muscle cells. We observed that the exposition of myocytes to aged, insulin resistant and adipocytes treated with

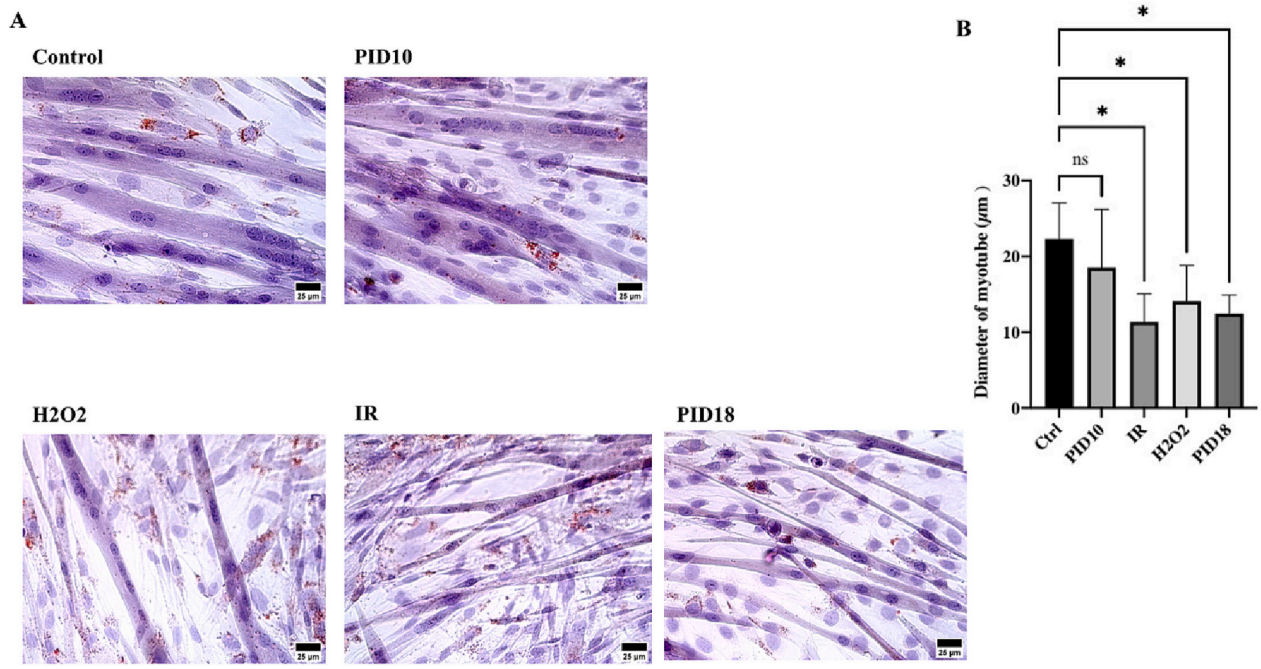

Fig. 4. Morphological changes of C2C12 myotubes after treatment with conditioned medium (CM) collected from adipocytes cultured under different experimental conditions. (A) Hematoxylin and Eosin, as well as Red Oil O staining, of C212 myotubes exposed to control medium and CM from adipocytes in various conditions, including adult adipocytes (PID10), reactive oxygen species treatment (H2O2), insulin-resistant adipocytes (IR), and aged adipocytes (PID18) (scale bar = 25 µm). (B) Diameter of myocyte fibers (µm) in C2C12 cells treated with control medium or CM from different adipocyte conditions. Data are presented as mean ± SD from three independent experiments. *p < 0.05 *vs.* the control, ns: Not Significant. PID: post induction day. (For interpretation of the references to colour in this figure legend, the reader is referred to the web version of this article.)

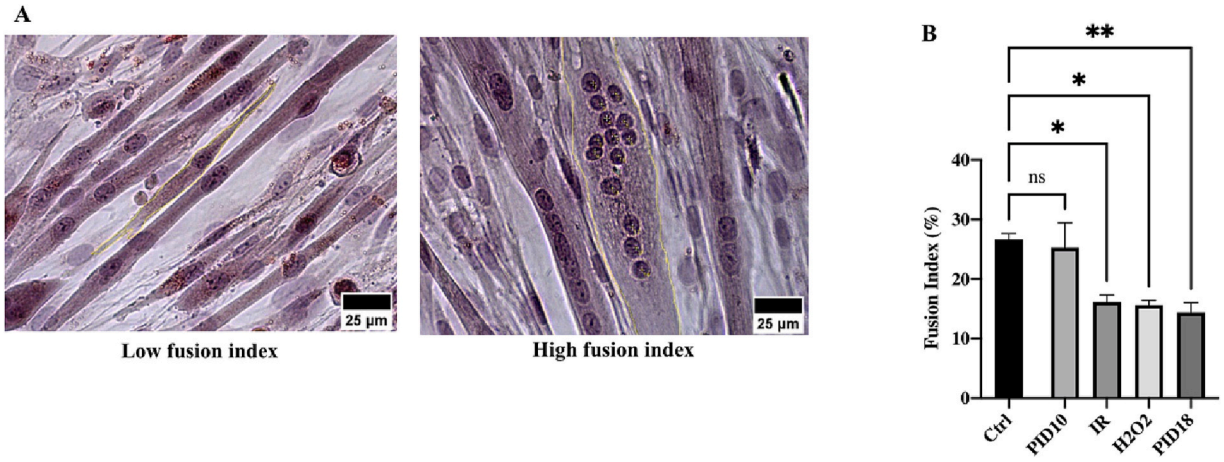

Fig. 5. Evaluation of differentiation grade by Fusion Index in C2C12 cells treated with conditioned medium (CM) from adipocytes under different experimental conditions. (A) Representative images showing low and high myotube Fusion Index (scale bar = 25 µm). (B) Fusion Index of C2C12 cells treated with control medium or CM from adult adipocytes (PID10), adipocytes treated with reactive oxygen species (H2O2), insulin-resistant adipocytes (IR), and aged adipocytes (PID18). Data are presented as mean ± SD from three independent experiments. *p < 0.05, **p < 0.01 *vs.* the control, ns: Not Significant. PID: post induction day.

reactive oxygen species, was linked to a reduction in myocytes differentiation, increased myotube atrophy, and to an activation of myostatin pathway.

In our *in vitro* model, from a morphological point of view, the crosstalk between myocytes and aged adipocytes was characterized by a greater degree of atrophy with a reduction in the diameters of myotubes and by an alteration of myotubes differentiation, compared to control myocytes. In previous studies a decrease in diameter and fusion index of myoblasts was described after co-culture with mature adipocytes (Dietze et al., 2002) or with adipocytes taken from the visceral AT of obese subjects (Pellegrinelli et al., 2015). Our data support also a role for aged or dysfunctional fat cells in the pathogenesis of muscle cells atrophy and show that oxidative stress or insulin resistance might also contribute to the onset of this process.

In parallel to these morphological findings, muscle cells treated with conditioned medium of aged adipocytes showed a tendential reduction in the expression of genes of myocellular differentiation and an increase in the expression of genes related to muscle atrophy.

Regarding genes related to muscle atrophy, we observed an increase in MuRF1 expression compared to control, after the treatment of muscle cells with conditioned medium of stressed adipocytes. These findings seem to be particularly relevant since MuRF1 is muscle-specific E3

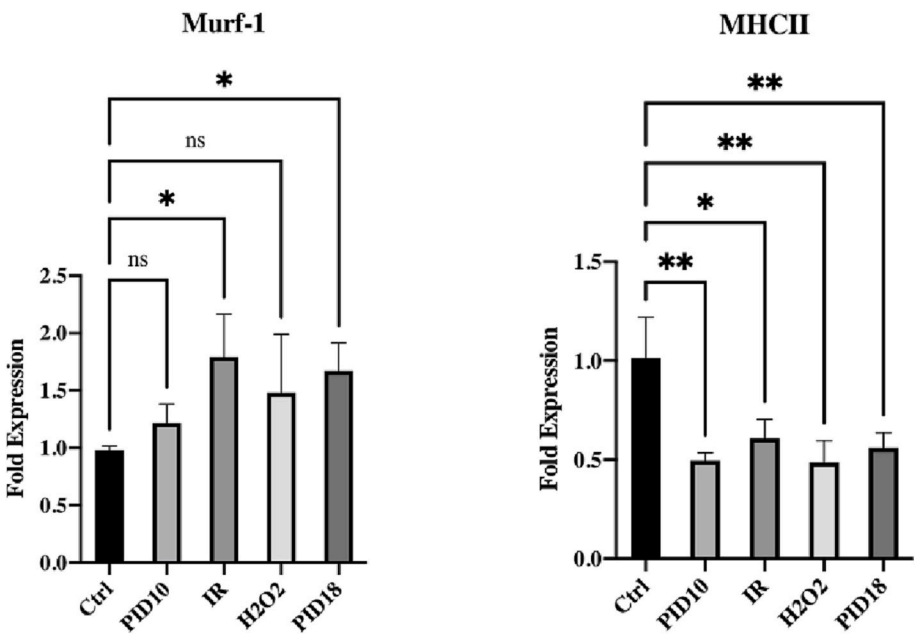

Fig. 6. Gene expression analysis was performed using RT-PCR to investigate the expression levels of MuRF1 and MHCII genes in C2C12 cells treated with conditioned medium (CM) obtained from adipocytes under different experimental conditions. MuRF1 gene expression, which is associated with muscle atrophy, and MHCII gene expression, serving as a marker for differentiated myotubes, were assessed in these myotubes. C2C12 cells were incubated with either the control medium or CM derived from adult adipocytes (PID10), adipocytes treated with reactive oxygen species (H2O2), insulin-resistant adipocytes (IR), and aged adipocytes (PID18). The data are presented as mean ± SD from three to five independent experiments. *p < 0.05, **p < 0,01 *vs.* the control, ns: Not Significant. PID: post induction day; MuRF1: Muscle RING Finger-1; MHCII: Myosin Heavy Chain II.

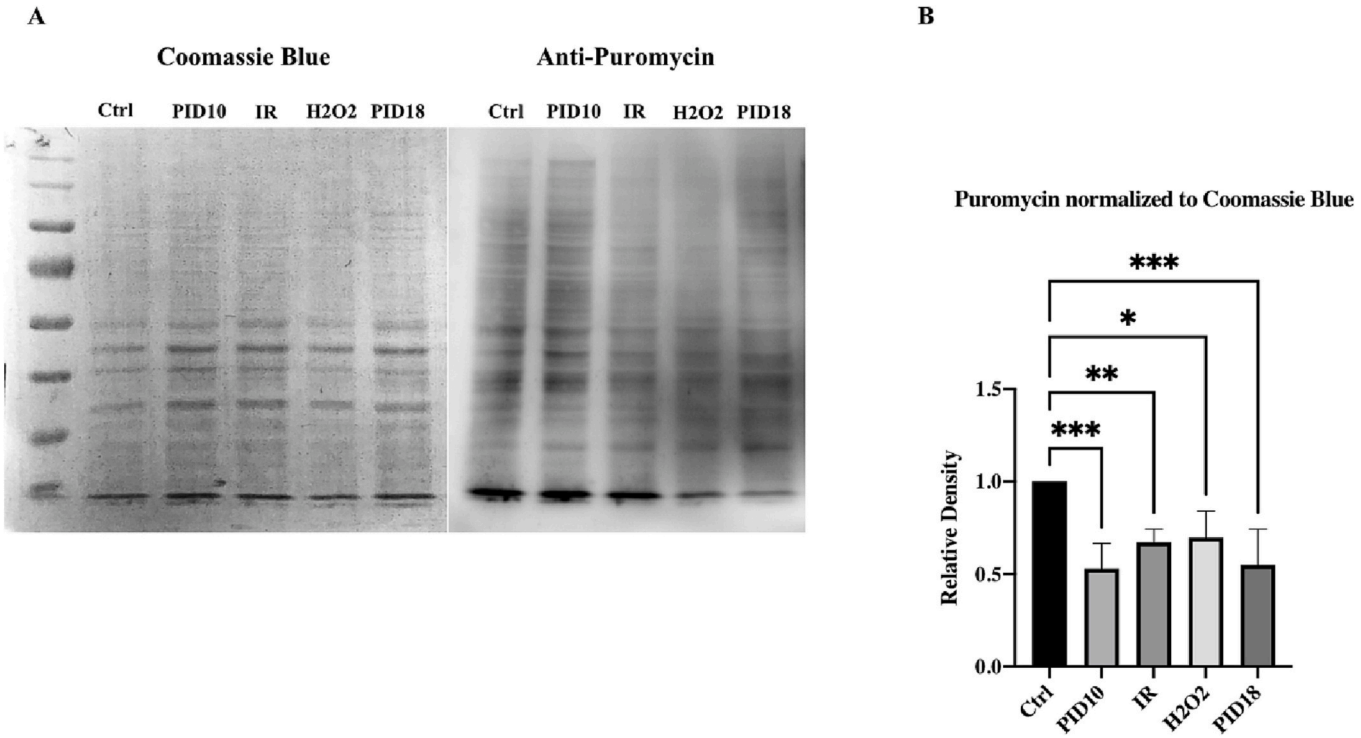

Fig. 7. Protein synthesis was assessed by puromycin incorporation in C2C12 cells treated with conditioned medium (CM) from adipocytes under different experimental conditions. Puromycin incorporation was performed using the SUnSET method described in Materials and Methods on C2C12 cells treated with the control medium or with CM from adult adipocytes (PID10), adipocytes treated with reactive oxygen species (H2O2), insulin-resistant adipocytes (IR), and aged adipocytes (PID18). (A) Representative image of Western blot analysis for puromycin with Coomassie Blue staining to ensure equal protein loading in the different experimental conditions. (B) Quantification of the puromycin-labeled peptides after normalization with Coomassie Blue staining. The data are presented as mean ± SD from four independent experiments. *p < 0.05, **p < 0,01, ***p < 0.001 *vs.* the control. PID: post induction day.

ubiquitin ligase, activated in different models of muscle atrophy, involved in muscle remodeling and metabolism (Foletta et al., 2011), known with the name of "atrogene" and considered as a marker of muscle atrophy (Bodine and Baehr, 2014).

As muscle atrophy interferes with the expression of many transcription factors and the age-related decrease in muscle mass derives not only from an increase in protein catabolism but also from reduced protein synthesis, in a contest of compromised muscle regeneration (Morley et al., 2001), we continued to examine the expression of genes of myocellular differentiation. We found that mRNA expression of MyhC-IIb, considered as a marker of the differentiated state (Agarwal et al., 2020), was significantly reduced after exposure to conditioned

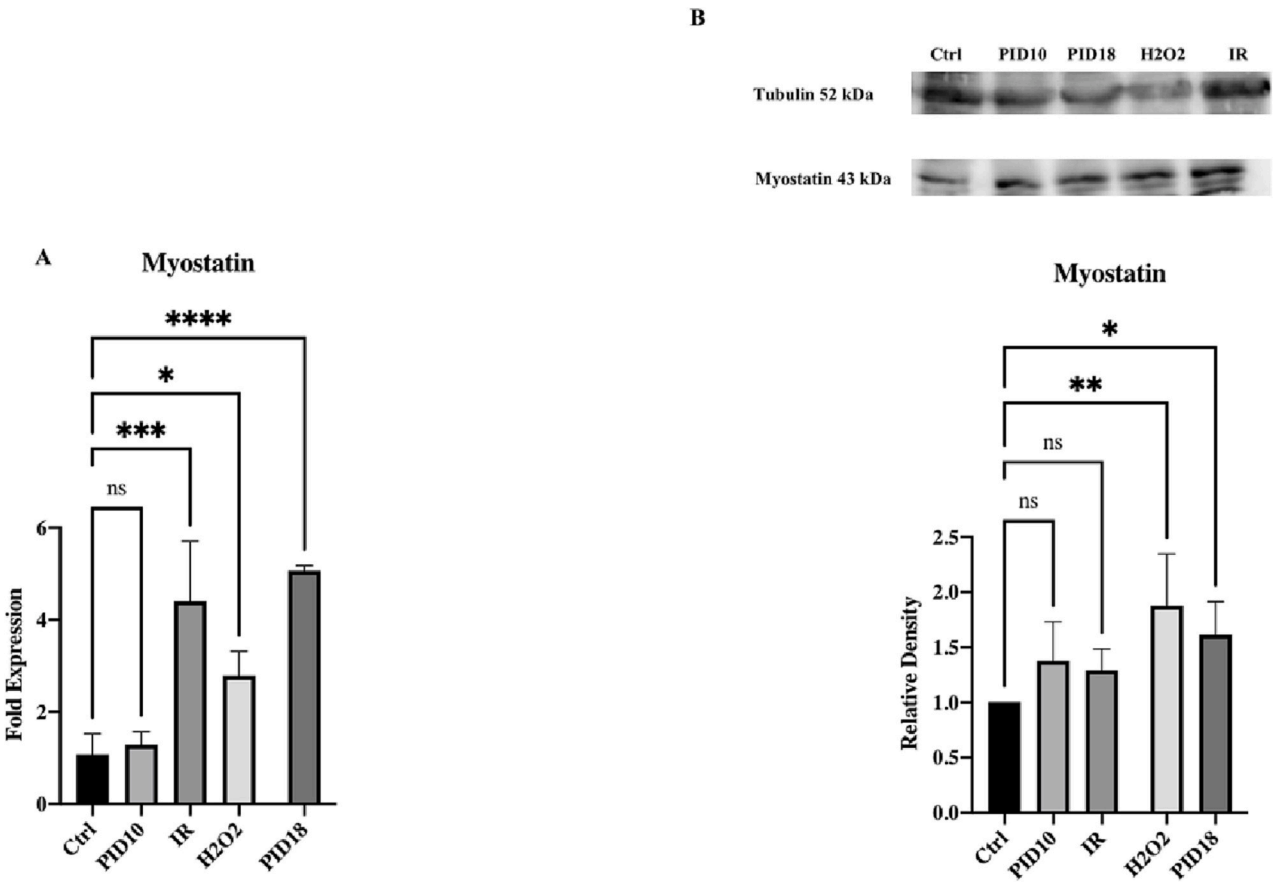

Fig. 8. Analysis of myostatin expression in C2C12 cells treated with conditioned medium (CM) from adipocytes under different experimental conditions. C2C12 cells were incubated with the control medium or with CM from adult adipocytes (PID10), adipocytes treated with reactive oxygen species (H2O2), insulin-resistant adipocytes (IR), and aged adipocytes (PID18). (A) Gene expression analysis of myostatin. Data are presented as mean ± SD from three independent experiments. (B) Western blotting assay of myostatin expression normalized to Alpha-Tubulin in C2C12 cells under the different experimental conditions. Cropped blots and densitometric analysis are shown. Data are presented as mean ± SD from five independent experiments. *p < 0.05, **p < 0.01, ***p < 0.001, ****$p < 0.0001$ *vs.* the control, ns: Not Significant, PID: post induction day.

media from all models of aged or stressed adipocytes.

In the view of our interest in the mechanisms associated with muscle mass, we performed WB-SUnSET as a method for assessing the level of protein synthesis in muscle cells. The results obtained in our study demonstrate a significant reduction in muscle anabolism, and the capacity of muscle cells to synthesize proteins, assessed by puromycin incorporation which was significantly declined when C2C12 cells were treated with the different conditioned medium from aged or stressed adipocytes.

These results are in line with previous studies by Kim et al. (2018) who found a reduction in the expression of MyoD and an increase in Atrogin-1, after treating myotubes with a pro-inflammatory mixture and also in agreement with the observations that co-cultures of myocytes with visceral fat cells of obese patients showed greater degree of atrophy in muscle and a diminished differentiation compared to myocytes co-cultured with the subcutaneous AT (Pellegrinelli et al., 2015). In fact, visceral fat is known for its greater pro-inflammatory profile than subcutaneous fat (Alvehus et al., 2010), thereby suggesting that inflammation could be one of the mechanisms for senescent or dysfunctional adipocytes in our *in vitro* model.

Actually, our experiment expands previous findings because to our knowledge, no study has specifically assessed the role of aged and senescent fat cells in the development of muscle atrophy. It is known that with aging, WAT becomes dysfunctional, showing an increased profile of pro-inflammatory adipokines produced by adipose cells and greater infiltration of inflammatory cells. Furthermore, senescent or stressed adipocytes have been shown to be characterized by an increase in pro-inflammatory mediators (Tchkonia et al., 2010). Accordingly, in this *in vitro* model we found a significant increase in gene expression of pro-inflammatory cytokines, in particular in adipocytes exposed to oxidative stress but also tendentially in the other conditions. We have already described a significant increase in IL-6 and decreased in adiponectin in aged cells (Zoico et al., 2019) and that dysfunctional adipocyte increased mRNA expression of some senescence-associated genes such as BCL-2, BAX and LITAF (Zoico et al., 2019), further supporting inflammation and senescence as important mechanisms involved in the crosstalk between muscle and fat compartments.

In our preliminary experiment, one of the most relevant results was the increased gene expression of myostatin in myocytes treated with the conditioned medium from aged fat cells and stressed adipocytes compared to control, suggesting a potential link between senescent and dysfunctional adipocytes and muscle atrophy. Moreover, gene expression of myostatin was also confirmed by Western blot analysis showing a statistically significant increment in myostatin level in myocytes treated with medium form aged adipocytes as well as from adipocytes exposed to oxidative stress.

Myostatin is a growth factor expressed in skeletal muscle and WAT necessary in the maintenance of muscle integrity. It down regulates muscle mass, causes atrophy (Lee, 2004), and negatively affects myoblasts differentiation and proliferation (Langley et al., 2002; Ríos et al., 2002). It is also involved in the metabolism of glucose and the inhibition of myostatin resulted in improved glucose metabolism and sensitivity (Guo et al., 2009). Myostatin may also decrease protein synthesis in differentiated myotubes (Taylor et al., 2001) regulating the activation of

the Akt/mTOR/p70S6 signaling, which mediates both the differentiation and hypertrophy of myotubes (Trendelenburg et al., 2009). An *in vitro* study on adult C2C12 showed that myostatin could reduce protein synthesis either affecting the mTORC pathway (Trendelenburg et al., 2009) or blocking eEF2K-eEF2 signaling (Deng et al., 2017). Therefore, our results globally suggest that senescent adipocytes could be important regulators of muscle integrity and in particular of muscle differentiation and proliferation also through myostatin modulation.

Myostatin is also known as a factor promoting fibrosis by increasing the synthesis of components of the extracellular matrix in muscle (Li et al., 2012). Unfortunately, our preliminary data are not stronger enough to support an increase of pro-fibrotic muscle biomarkers after treatment with conditioned medium from dysfunctional adipocytes. However, our *in vitro* experiment was not specifically design to study muscle fibrosis which should be better explored by *in vivo* studies with muscle biopsies or by more complex *in vitro* experiments mimicking the complexity of tissues.

Interestingly other muscular pathways, besides myostatin, are emerging as potentially involved in muscle fibrosis and muscle dysfunction of aging. CCN-2 has been shown to have a robust pro-fibrotic effect, as confirmed also by the fact that its inhibition is sufficient to improve the phenotype of fibrotic muscle (Gonzalez and Brandan, 2019; Morales et al., 2013; Rebolledo et al., 2019). CCN-2 has also been found to be increased in some models of Sarcopenia, and might negatively affect muscle regeneration (Nishida et al., 2015).

All together our data show that aged and dysfunctional adipocytes may contribute to the development of age-related muscle mass reduction and dysfunction.

Aged adipocytes could thus represent a potential target to reduce the adverse effects on the muscle of senescent and dysfunctional adipocytes. Recently a new class of compounds, called senolytics, have been studied to selectively clear senescent cells in different tissues (Xu et al., 2018). Only a few substances have been tested for WAT. Among them, the polyphenol quercetin has been shown to have a senolytic effect on WAT, either *in* vitro or *in vivo* experiments (Kobori et al., 2016; Yang et al., 2008). In mice subjected to a high-fat diet with or without supplementation with quercetin, quercetin reduced inflammatory cytokine levels and macrophage accumulation in the skeletal muscle, reduced the expression of Atrogin-1 and MuRF1, protecting animals from a reduction in muscle mass and diameters of muscle fibers (Le et al., 2014). Although some *in vitro* studies hypothesize a direct action of quercetin on muscle cells, it cannot be ruled out an effect of this molecule also on WAT infiltrating the muscle with a selective action on senescent adipocytes.

Finally, in interpreting our results, some intrinsic limitations of the adopted study model should be recognized. WAT and muscle are composed of different cell types, adipocytes and myocytes, and the complexity of the tissue and the interactions between all their components cannot be studied just through *in vitro* models. Moreover, evaluation of fibrosis is challenging to perform *in vitro* and requires animal and human studies with biopsy specimens. The data from this study need to be confirmed with further analyses, possibly in cultures of human adipocytes and myocytes and through modulation of some pathways to further support the role of the senescent adipocyte in the pathophysiology of muscle aging.

5. Conclusion

In conclusion our study suggests that aged and senescent adipocytes might be involved in a paracrine network with muscle, negatively influencing myocytes trophism, function, and regenerative capacity. Inflammation, SASP and oxidative stress, characterizing aged adipocytes, might affect myocytes homeostasis increasing the expression of myostatin. The pathways activated could lead to muscle differentiation inhibition and enhanced muscle atrophy. Further studies are needed to clarify if the age and obesity-related reduction in mass, quality and performance of muscle cells might be arrested by the treatment of dysfunctional WAT and if senescent adipocytes could be not only effectors but also potential targets to counteract muscle cells dysfunction.

Funding

This project was supported by grants from Fondazione Cariplo (2016-1006 to ZM).

Contribution to the field statement

Adipose tissue dysfunction characterizing obesity and aging might affect muscle integrity and function, leading to its degeneration and contributing to the pathogenesis of Sarcopenia. In particular, aged and senescent adipocytes might be involved in a paracrine network with muscle that could negatively influence myocytes trophism, function, and regenerative capacity. Inflammation, SASP and oxidative stress, characterizing aged adipocytes, might affect myocytes homeostasis increasing the expression of myostatin. The pathways activated could lead to muscle differentiation inhibition, increase fibrosis and enhanced muscle atrophy. Senescent adipocytes could be not only effectors but also potential targets to counteract muscle cells dysfunction.

CRediT authorship contribution statement

Zoico Elena: Conceptualization, Formal analysis, Writing-Original and revised Draft.
Saatchi Tanaz: Conceptualization, Methodology, Investigation, Writing-Original and revised Draft.
Nori Nicole: Resources.
Mazzali Gloria: Writing-Original Draft.
Rizzatti Vanni: Methodology, Validation.
Pizzi Eleonora: Investigation.
Fantin Francesco: Formal analysis.
Giani Anna: Writing - Original Draft.
Urbani Silvia: Visualization.
Zamboni Mauro: Conceptualization, Supervision, Funding acquisition, Writing-Original Draft.

Declaration of competing interest

The authors declare that the research was conducted in the absence of any commercial or financial relationship that could be construed as a potential conflict of interest.

Data availability

Data will be made available on request.

Acknowledgements

We thank the staff of the Research Center LURM, as well as of the CPT (Technology Platform Center), for the precious support during the experimental research.

Appendix A. Supplementary data

Supplementary data to this article can be found online at https://doi.org/10.1016/j.exger.2023.112233.

References

Agarwal, M., Sharma, A., Kumar, P., Kumar, A., Bharadwaj, A., Saini, M., Kardon, G., Mathew, S.J., 2020. Myosin heavy chain-embryonic regulates skeletal muscle differentiation during mammalian development. Development (Cambridge, England) 147 (7), dev184507.
Alvehus, M., Burén, J., Sjöström, M., Goedecke, J., Olsson, T., 2010. The human visceral fat depot has a unique inflammatory profile. Obesity 18 (5), 879–883.

Bodine, S.C., Baehr, L.M., 2014. Skeletal muscle atrophy and the E3 ubiquitin ligases MuRF1 and MAFbx/atrogin-1. Am. J. Physiol. Endocrinol. Metab. 307 (6), E469–E484.
Deng, Z., Luo, P., Lai, W., Song, T., Peng, J., Wei, H.-K., 2017. Myostatin inhibits eEF2K-eEF2 by regulating AMPK to suppress protein synthesis. Biochem. Biophys. Res. Commun. 494 (1), 278–284.
Dietze, D., Koenen, M., Röhrig, K., Horikoshi, H., Hauner, H., Eckel, J., 2002. Impairment of insulin signaling in human skeletal muscle cells by co-culture with human adipocytes. Diabetes 51 (8), 2369–2376.
Foletta, V.C., White, L.J., Larsen, A.E., Léger, B., Russell, A.P., 2011. The role and regulation of MAFbx/atrogin-1 and MuRF1 in skeletal muscle atrophy. Pflugers Arch. - Eur. J. Physiol. 461 (3), 325–335.
Franceschi, C., Campisi, J., 2014. Chronic inflammation (inflammaging) and its potential contribution to age-associated diseases. J. Gerontol. A Biol. Sci. Med. Sci. 69 (Suppl_1), S4–S9.
Gallagher, D., Kuznia, P., Heshka, S., Albu, J., Heymsfield, S.B., Goodpaster, B., et al., 2005. Adipose tissue in muscle: a novel depot similar in size to visceral adipose tissue. Am. J. Clin. Nutr. 81 (4), 903–910.
Gonzalez, D., Brandan, E., 2019. CTGF/CCN2 from skeletal muscle to nervous system: impact on neurodegenerative diseases. Mol. Neurobiol. 56 (8), 5911–5916.
Goodpaster, B.H., He, J., Watkins, S., Kelley, D.E., 2001. Skeletal muscle lipid content and insulin resistance: evidence for a paradox in endurance-trained athletes. J. Clin. Endocrinol. Metab. 86 (12), 5755–5761.
Guo, T., Jou, W., Chanturiya, T., Portas, J., Gavrilova, O., McPherron, A.C., 2009. Myostatin inhibition in muscle, but not adipose tissue, decreases fat mass and improves insulin sensitivity. PLoS One 4 (3), e4937.
Kalinkovich, A., Livshits, G., 2017. Sarcopenic obesity or obese sarcopenia: a cross talk between age-associated adipose tissue and skeletal muscle inflammation as a main mechanism of the pathogenesis. Ageing Res. Rev. 35, 200–221.
Kim, S., Lee, M.-J., Choi, J.-Y., Park, D.-H., Kwak, H.-B., Moon, S., et al., 2018. Roles of exosome-like vesicles released from inflammatory C2C12 myotubes: regulation of myocyte differentiation and Myokine expression. Cell. Physiol. Biochem. 48 (5), 1829–1842.
Kobori, M., Takahashi, Y., Sakurai, M., Akimoto, Y., Tsushida, T., Oike, H., et al., 2016. Quercetin suppresses immune cell accumulation and improves mitochondrial gene expression in adipose tissue of diet-induced obese mice. Mol. Nutr. Food Res. 60 (2), 300–312.
Langley, B., Thomas, M., Bishop, A., Sharma, M., Gilmour, S., Kambadur, R., 2002. Myostatin inhibits myoblast differentiation by Down-regulating MyoD expression*. J. Biol. Chem. 277 (51), 49831–49840.
Le, N.H., Kim, C.-S., Park, T., Park, J.H.Y., Sung, M.-K., Lee, D.G., et al., 2014. Quercetin protects against obesity-induced skeletal muscle inflammation and atrophy. Mediat. Inflamm. 2014, e834294.
Lee, S.-J., 2004. Regulation of muscle mass by Myostatin. Annu. Rev. Cell Dev. Biol. 20 (1), 61–86.
Li, Z.B., Zhang, J., Wagner, K.R., 2012. Inhibition of myostatin reverses muscle fibrosis through apoptosis. J. Cell Sci. 125 (17), 3957–3965.
Morales, M.G., Cabrera, D., Céspedes, C., Vio, C.P., Vazquez, Y., Brandan, E., et al., 2013. Inhibition of the angiotensin-converting enzyme decreases skeletal muscle fibrosis in dystrophic mice by a diminution in the expression and activity of connective tissue growth factor (CTGF/CCN-2). Cell Tissue Res. 353 (1), 173–187.
Morley, J.E., Baumgartner, R.N., Roubenoff, R., Mayer, J., Nair, K.S., 2001. Sarcopenia. J. Lab. Clin. Med. 137 (4), 231–243.
Nishida, T., Kubota, S., Aoyama, E., Janune, D., Lyons, K.M., Takigawa, M., 2015. CCN family protein 2 (CCN2) promotes the early differentiation, but inhibits the terminal differentiation of skeletal myoblasts. J. Biochem. 157 (2), 91–100.
Palmer, A.K., Kirkland, J.L., 2016. Aging and adipose tissue: potential interventions for diabetes and regenerative medicine. Exp. Gerontol. 86, 97–105.
Pedersen, B.K., 2011. Muscles and their myokines. J. Exp. Biol. 214 (2), 337–346.
Pellegrinelli, V., Rouault, C., Rodriguez-Cuenca, S., Albert, V., Edom-Vovard, F., Vidal-Puig, A., et al., 2015. Human adipocytes induce inflammation and atrophy in muscle cells during obesity. Diabetes 64 (9), 3121–3134.
Petersen, K.F., Befroy, D., Dufour, S., Dziura, J., Ariyan, C., Rothman, D.L., et al., 2003. Mitochondrial dysfunction in the elderly: possible role in insulin resistance. Science 300 (5622), 1140–1142.
Pinel, A., Rigaudière, J.-P., Jouve, C., Capel, F., 2018. Modulation of insulin resistance and the adipocyte-skeletal muscle cell cross-talk by LCn-3PUFA. Int. J. Mol. Sci. 19 (9).
Rebolledo, D.L., González, D., Faundez-Contreras, J., Contreras, O., Vio, C.P., Murphy-Ullrich, J.E., et al., 2019. Denervation-induced skeletal muscle fibrosis is mediated by CTGF/CCN2 independently of TGF-β. Matrix Biol. 82, 20–37.
Ríos, R., Carneiro, I., Arce, V.M., Devesa, J., 2002. Myostatin is an inhibitor of myogenic differentiation. Am. J. Phys. Cell Phys. 282 (5), C993–C999.
Sell, H., Eckardt, K., Taube, A., Tews, D., Gurgui, M., Van Echten-Deckert, G., et al., 2008. Skeletal muscle insulin resistance induced by adipocyte-conditioned medium: underlying mechanisms and reversibility. Am. J. Physiol. Endocrinol. Metab. 294 (6), E1070–E1077.
Taylor, W.E., Bhasin, S., Artaza, J., Byhower, F., Azam, M., Willard, D.H., et al., 2001. Myostatin inhibits cell proliferation and protein synthesis in C2C12 muscle cells. Am. J. Physiol. Endocrinol. Metab. 280 (2), E221–E228.
Tchkonia, T., Morbeck, D.E., Zglinicki, T.V., Deursen, J.V., Lustgarten, J., Scrable, H., et al., 2010. Fat tissue, aging, and cellular senescence. Aging Cell 9 (5), 667–684.
Trendelenburg, A.U., Meyer, A., Rohner, D., Boyle, J., Hatakeyama, S., Glass, D.J., 2009. Myostatin reduces Akt/TORC1/p70S6K signaling, inhibiting myoblast differentiation and myotube size. Am. J. Phys. Cell Phys. 296 (6), C1258–C1270.
Visser, M., Goodpaster, B.H., Kritchevsky, S.B., Newman, A.B., Nevitt, M., Rubin, S.M., et al., 2005. Muscle mass, muscle strength, and muscle fat infiltration as predictors of incident mobility limitations in well-functioning older persons. J. Gerontol. Ser. A Biol. Med. Sci. 60 (3), 324–333.
Wilhelmsen, A., Tsintzas, K., Jones, S.W., 2021. Recent advances and future avenues in understanding the role of adipose tissue cross talk in mediating skeletal muscle mass and function with ageing. GeroScience 43 (1), 85–110.
Xu, M., Pirtskhalava, T., Farr, J.N., Weigand, B.M., Palmer, A.K., Weivoda, M.M., et al., 2018. Senolytics improve physical function and increase lifespan in old age. Nat. Med. 24 (8), 1246–1256.
Yang, J.-Y., Della-Fera, M.A., Rayalam, S., Ambati, S., Hartzell, D.L., Park, H.J., et al., 2008. Enhanced inhibition of adipogenesis and induction of apoptosis in 3T3-L1 adipocytes with combinations of resveratrol and quercetin. Life Sci. 82 (19), 1032–1039.
Yu, Y.-H., Zhu, H., 2004. Chronological changes in metabolism and functions of cultured adipocytes: a hypothesis for cell aging in mature adipocytes. Am. J. Physiol. Endocrinol. Metab. 286 (3), E402–E410.
Zamboni, M., Nori, N., Brunelli, A., Zoico, E., 2021. How does adipose tissue contribute to inflammageing? Exp. Gerontol. 143, 111162.
Zoico, E., Di Francesco, V., Olioso, D., Fratta Pasini, A.M., Sepe, A., Bosello, O., Cinti, S., Cominacini, L., Zamboni, M., 2010. In vitro aging of 3T3-L1 mouse adipocytes leads to altered metabolism and response to inflammation. Biogerontology 11 (1), 111–122.
Zoico, E., Corzato, F., Bambace, C., Rossi, A.P., Micciolo, R., Cinti, S., et al., 2013. Myosteatosis and myofibrosis: relationship with aging, inflammation, and insulin resistance. Arch. Gerontol. Geriatr. 57 (3), 411–416.
Zoico, E., Rizzatti, V., Policastro, G., Tebon, M., Darra, E., Rossi, A.P., et al., 2019. In vitro model of chronological aging of adipocytes: interrelationships with hypoxia and oxidation. Exp. Gerontol. 121, 81–90.